



Letter

Nanostructure stabilization in electrodeposited Al–Mg dendrites



A B S T R A C T

Keywords:

Al–Mg
Electrodeposition
Nanostructure
Stabilization
Segregation

Electrodeposited Al–Mg dendrites with globular morphology exhibited core–shell (coarse–fine) type microstructure with grain sizes ~100 and ~16 nm, respectively. The grain boundary and grain compositions of core are ~10 and ~6 at.% Mg, respectively. Those of shell are ~36 and ~20 at.% Mg, respectively. The excess Mg ratio at boundaries of shell and core ($\Gamma_{Mg, fine}/\Gamma_{Mg, coarse}$) is 1.17:1. This relative grain boundary segregation of Mg decreases the grain boundary energy from coarse to fine region and can result in nanostructure stabilization of fine shell at ~16 nm.

© 2016 Elsevier B.V. All rights reserved.

1. Introduction

The large fraction of high energy grain boundaries renders nanocrystalline materials highly unstable. Strategies for nanostructure stabilization include adding second-phase materials, solute atoms etc. E.g. Ru–Al [1], Y–Fe [2], Ni–P [3,4], Ni–W [5].

The solute atom for nanostructure stabilization is chosen based on (i) solubility in matrix; (ii) segregation energy [1]. The lower solubility and higher segregation energy result in higher solute segregation tendency towards grain boundaries causing nanostructure stabilization. E.g. Ni–P system exhibits negligible solubility of P in Ni and the segregation energy: 100 kJ/mol [3]. Stable nanograins (5 nm) were obtained with P-rich grain boundaries and P-poor grains. Similarly, 1–27 at.%W in Ni produced stable nanograins (140–2 nm) by electrodeposition [5].

Thermodynamically, nanostructure stabilization requires a reduction of (i) total system free energy ($\Delta G < 0$) and (ii) Grain boundary energy (GBE) ($\Delta\gamma < 0$). γ depends on the excess grain boundary solute concentration (Γ) through Gibbs adsorption isotherm (Eq. (1)) [1]:

$$\gamma = \gamma_0 - \Gamma(G_{seg} + RT \ln x_g) \quad (1)$$

where γ_0 : GBE of pure polycrystalline matrix; x_g : grain solute composition; and G_{seg} : segregation energy. Usually higher G_{seg} renders easier nanostructure stabilization (E.g. Ni–P [3]).

Interestingly, we demonstrate that nanostructure stabilization can occur even in Al–Mg system exhibiting moderate segregation energy of 18 kJ/mol [6]. Al–Mg alloys are employed in propellants in aerospace industry for their high volumetric heat [7]. Their excellent corrosion resistance renders them as coating materials in automobile industry [8]. MgH_2 is a promising hydrogen storage material. Al can improve its oxidation resistance [9], heat conductivity [10], and decrease its dehydrogenation temperature [11].

We electrodeposited nanocrystalline supersaturated metastable

Al–Mg dendrites for H_2 -storage [12]. By thorough analyses we understood the Al–Mg electrodeposition scheme [13]; internal [14], external morphological [12], microstructural [15], compositional [16,17], textural [18], phase [19] features; and the dendritic growth mechanisms [20,21]. The dendrites exhibited core–shell (coarse–fine) microstructure with the core and shell grain sizes of ~100 and ~16 nm, respectively. The nanostructure stabilization in fine shell is understood through the relative grain boundary segregation tendency of Mg ($\Gamma_{Mg, fine}/\Gamma_{Mg, coarse}$) and the reduced GBE from coarse to fine structure ($\Delta\gamma = \gamma_{fine} - \gamma_{coarse}$).

2. Experimental procedure

Al–Mg dendrites were galvanostatically electrodeposited using an organometallic-based electrolyte: $Na[Al(C_2H_5)_4] + 2Na[(C_2H_5)_3Al-H-Al(C_2H_5)_3] + 2.5Al(C_2H_5)_3 + 6$ toluene at 90 °C and current density of 60 mA cm⁻² [12]. Mg was introduced into the electrolyte by Mg anode through “pre-electrodeposition” for 90 min ensuring Mg saturation in the electrolyte and eventually electrodeposition was conducted [13]. The deposits were cleaned [12] and characterized using JEOL 6335F Field emission gun scanning electron microscope (SEM) for morphology and APD XRD 3720 for phases. JEOL 2010F transmission electron microscope (TEM) with 0.5 nm Scanning TEM (STEM) spatial resolution, and energy dispersive spectroscopy (EDS) was employed for microstructural and compositional characterization. The longitudinal dendritic slices of 50–80 nm thickness were prepared by embedding the dendrites in SPI-PON 812 resin, and cutting by Leica Ultracut UCT ultramicrotome at 100 mm/s. The grain sizes were estimated using dark field imaging over 300 instances of grains.

3. Results and discussion

Fig. 1(a) shows the as-deposited Al–Mg globular dendrites

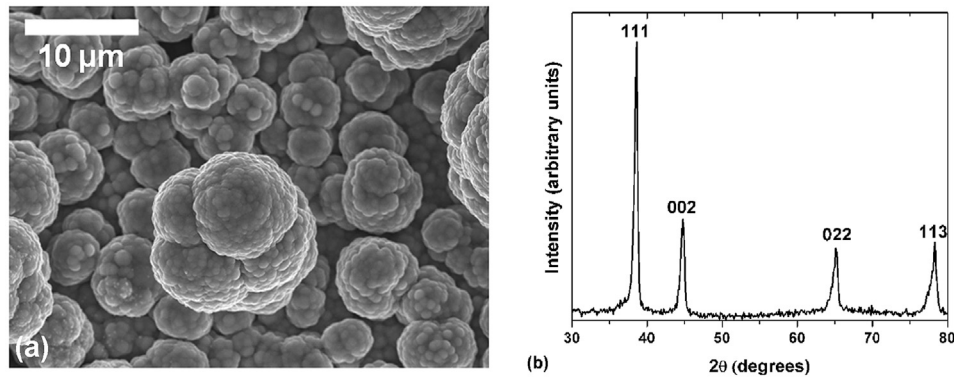


Fig. 1. (a) SEM image showing globular morphology, (b) XRD profile with fcc-Al(Mg) phase of Al–Mg dendrites.

assembled in stacks, suggesting non-equilibrium electrodeposition [12]. The XRD profile indicates face centered cubic (fcc)–Al(Mg) phase of these dendrites (Fig. 1b).

Fig. 2(a) presents a dendritic longitudinal section along its growth direction. The globules possess coarse core (grain size ~100 nm) enveloped by fine shell (grain size ~16 nm) [15], demarcated by dashed boundary. Fig. 2(b) indicates the *trans*-boundary global composition variation. The representative core and shell global compositions are ~6 and 10 at.% Mg, respectively. Since the slice thickness was ~50–80 nm, the compositions were corrected for absorption and fluorescence effects. From the results, the higher global composition results in the lower grain size.

Fig. 3(a) shows a coarse grain with composition line scan (at.% Mg) through it. The spotty selected area diffraction (SAED) pattern of Fig. 3(a) (inset, Fig. 3(b)), suggested the presence of a very few grains, confirmed by the dark field (DF) image in Fig. 3(b). Several contours within the grain are mostly due to the highly stressed nature of grain from non-equilibrium electrodeposition. The line scan indicates that composition was higher at boundaries and lower at grain interior (Fig. 3(a)). The representative compositions in the grain interior and boundary are ~6 and 10 at.% Mg, respectively (Fig. 3(c)).

Fig. 4(a) shows the composition line scan across a fine grain (~16 nm). The spotty SAED pattern (Fig. 4(b)) suggests mostly a single grain. The line scan in Fig. 4(a) shows that Mg is higher at boundary and lower within grain. The representative compositions within the grain and at boundary are ~20 and ~36 at.% Mg, respectively (Fig. 4(c)).

From the compositional information, the excess solute (Mg) at the grain boundaries was calculated using Gibbs–Duhem equation: $\Gamma_{Mg} = \frac{1}{a} [N_{b,Mg} - (N_{b,Al} \times N_{g,Mg}/N_{g,Al})]$ where, N_{ij} : amount of j th species (Al/Mg) at i th location (g : grain, b : boundary); a_i : grain boundary area [1]. The second term in brackets indicates the grain boundary Mg content proportional to that in the grains. The estimated grain boundary excess Mg of both the coarse and fine regions are: $\Gamma_{Mg,coarse} = 4.26/a_{coarse}$ and $\Gamma_{Mg,fine} = 20/a_{fine}$, respectively. a_{coarse} and a_{fine} : grain boundary areas of coarse and fine grained regions, respectively. $\Gamma_{Mg,fine}/\Gamma_{Mg,coarse}$ gives the relative grain boundary segregation of Mg in fine and coarse regions, which was estimated by considering a_{fine}/a_{coarse} . Dividing a 100×100 nm square into 6 nm square regions with lines of constant thickness, a_{fine}/a_{coarse} is 4:1. Hence, $\Gamma_{Mg,fine}/\Gamma_{Mg,coarse} = 1.17:1$. The relative grain boundary segregation of Mg and the microstructural studies suggest that solute (Mg) segregation (i) in fine region is subtly more than that in the coarse region; (ii) leads to nanostructure stabilization of the fine region (~16 nm, Fig. 4a).

The solute grain boundary segregation tendency depends on (i) solute solubility in matrix; (ii) segregation energy. The Al–Mg system exhibits <1 at.% mutual solubility at equilibrium [22] and moderate segregation energy (18 kJ/mol) [6]. Hence, Al–Mg exhibits lower solute segregation tendency than Ni–P (segregation energy 100 kJ/mol). Moreover, the increased Mg solubility (~20 at.% Mg, Fig. 2b) in Al, due to non-equilibrium electrodeposition, results in only a subtly more segregation of Mg in the fine region ($\Gamma_{Mg,fine}/\Gamma_{Mg,coarse} = 1.17:1$). This subtle segregation stabilized the grain size in fine region at ~16 nm (Fig. 4a).

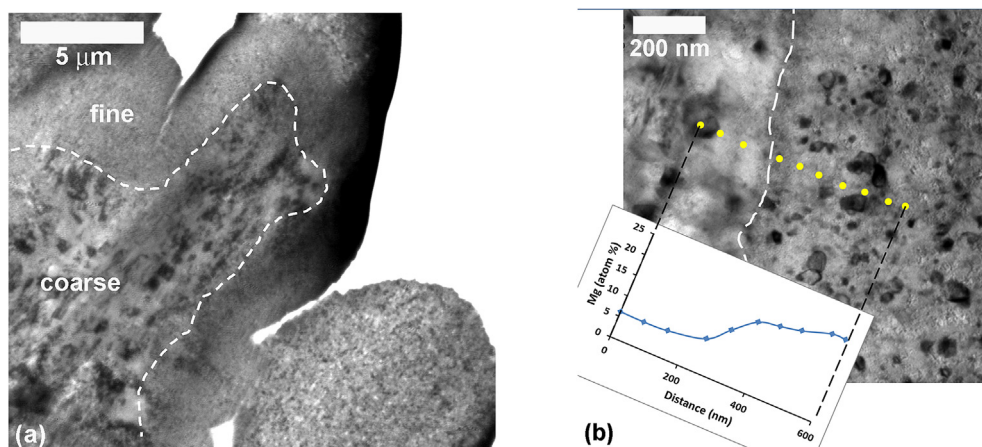


Fig. 2. TEM image showing (a) coarse–fine structure, (b) Composition variation across coarse–fine boundary in a dendrite.

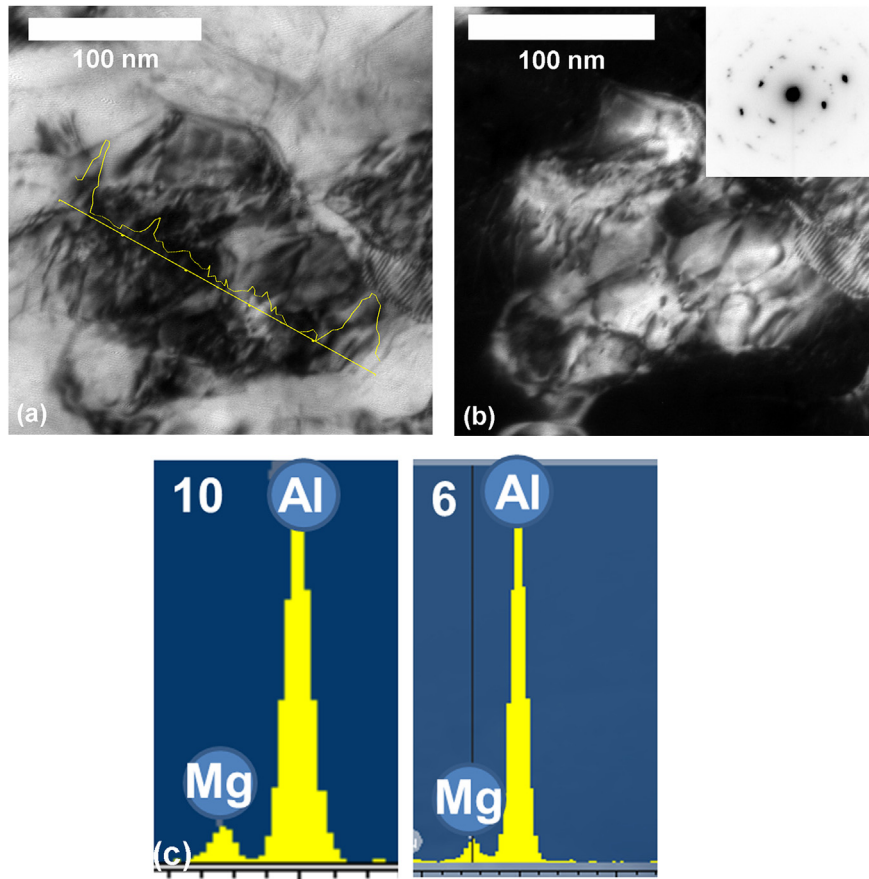


Fig. 3. (a) Bright field TEM image of coarse grain with composition line scan; (b) Dark field image of (a) with SAED pattern (inset); (c) EDS spectra showing representative grain boundary and interior compositions in coarse region.

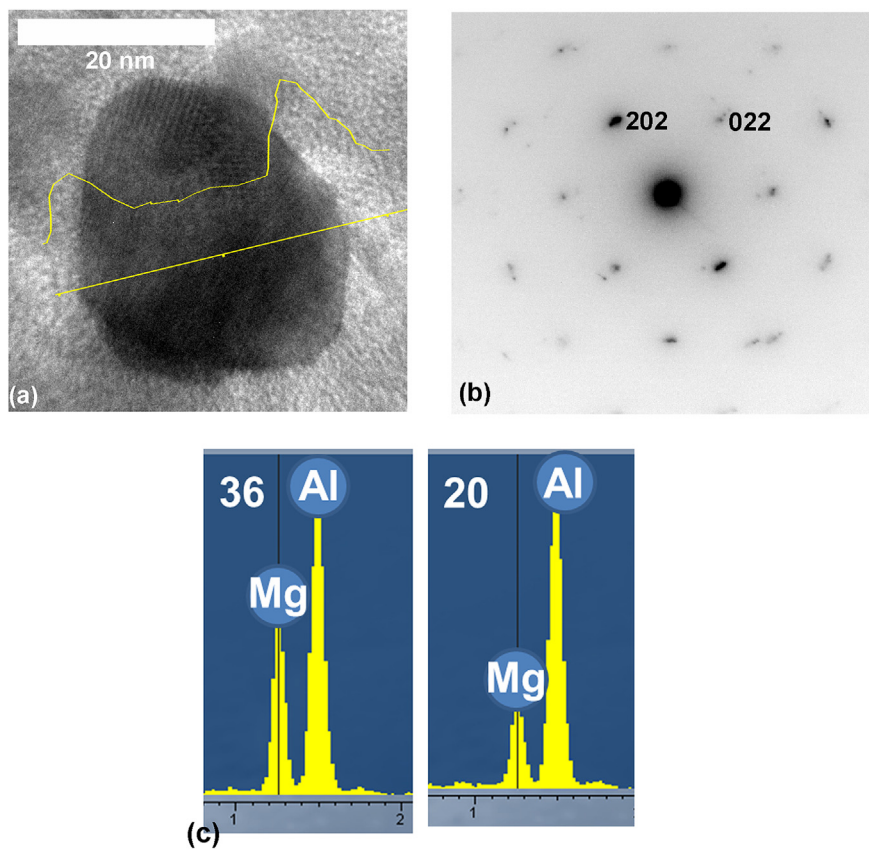


Fig. 4. (a) Bright field TEM image of fine grain with composition line scan; (b) SAED pattern of (a); (c) EDS spectra showing representative grain boundary and interior compositions in fine region.

Nanostructure stabilization in the fine region is understood by the Gibbs free energy change from coarse to fine region (ΔG). Pure nanocrystalline materials with large grain boundary fraction are unstable ($\Delta G > 0$). Hence, for nanostructure stabilization ΔG must be < 0 . However, $\Delta G = \Delta \gamma da$ at constant pressure and temperature, where $\Delta \gamma$ is the GBE change from coarse to fine region. $\Delta \gamma$ is estimated from Gibbs adsorption isotherm for Al–Mg system as $\gamma = \gamma_0 - \Gamma_{\text{Mg}}(G_{\text{seg}} + RT \ln x_{\text{g,Mg}})$ [1], where γ_0 : GBE of pure polycrystalline Al; G_{seg} : segregation energy; and $x_{\text{g,Mg}}$: Mg composition at grain ($= 0.06$ for coarse and 0.20 for fine, Figs. 3c and 4c). Writing separate expressions for γ_{coarse} and γ_{fine} and estimating their difference $\Delta \gamma = \gamma_{\text{fine}} - \gamma_{\text{coarse}}$ yields Eq. (2).

$$\Delta \gamma = \left[\frac{32.2}{a_{\text{fine}}} - \frac{12}{a_{\text{coarse}}} \right] RT - \left[\frac{20}{a_{\text{fine}}} - \frac{4.26}{a_{\text{coarse}}} \right] G_{\text{seg}} \quad (2)$$

Assuming $a_{\text{fine}}/a_{\text{coarse}} = 4:1$, the first term in Eq. (2) is < 0 and the second term is > 0 , rendering $\Delta \gamma < 0$. Therefore, $\Delta G = \Delta \gamma da < 0$ for grain refinement (since $da > 0$) as in the present case from coarse to fine region. Thus, the total free energy of the system from coarse to fine region is decreased explaining the stabilized nanostructure at ~ 16 nm (fine shell).

The present work demonstrates that even subtle solute segregation can cause nanostructure stabilization in electrodeposited Al–Mg dendrites.

4. Conclusions

Nanocrystalline Al–Mg dendrites with globular morphology were electrodeposited. The dendrites possessed core–shell type microstructure with coarse (core) and fine (shell) grain sizes of ~ 100 and ~ 16 nm, respectively. The grain boundary and grain compositions of core are ~ 10 and ~ 6 at.% Mg, respectively; those of the shell are ~ 36 and ~ 20 at.% Mg, respectively. The relative grain boundary segregation (ratio of excess Mg at boundaries of shell and core) is $\Gamma_{\text{Mg,fine}}/\Gamma_{\text{Mg,coarse}} = 1.17:1$. This subtle grain boundary segregation reduced the GBE ($\Delta \gamma < 0$) from coarse to fine structure. The decreased γ rendered nanostructure stabilization of the grain size at ~ 16 nm (fine shell).

Acknowledgments

This work was supported by National Science Foundation [grant number DMR–0605406].

References

[5] A.J. Detor, C.A. Schuh, Tailoring and patterning the grain size of

- nanocrystalline alloys, *Acta Mater.* 55 (2007) 371–379.
- [6] X. Liu, X. Wang, J. Wang, H. Zhang, First-principles investigation of Mg segregation at $\Sigma = 11(113)$ grain boundaries in Al, *J. Phys. Condens. Matter* 17 (2005) 4301–4308.
- [7] E.L. Dreizin, Experimental study of aluminum particle flame evolution in normal and micro-gravity, *Combust. Flame* 116 (1999) 323–333.
- [8] H. Lehmkuhl, K. Mehler, B. Reinhold, H. Bongard, B. Tesche, Deposition of aluminum-magnesium alloys from electrolytes containing organo-aluminum complexes, *Adv. Eng. Mater.* 3 (2001) 412–417.
- [9] A. Andreasen, M.B. Sorensen, R. Burkarl, B. Moller, A.M. Molenbroek, A.S. Pedersen, Interaction of hydrogen with an Mg–Al alloy, *J. Alloys Compd.* 404 (2005) 323–326.
- [10] A. Zaluska, L. Zaluski, J.O. Strom-Olsen, Structure, catalysis and atomic reactions on the nano-scale: a systematic approach to metal hydrides for hydrogen storage, *Appl. Phys. A* 72 (2001) 157–165.
- [11] M. Tanniru, F. Ebrahimi, Effect of Al on the hydrogenation characteristics of nanocrystalline Mg powder, *Int. J. Hydrogen Energy* 34 (2009) 7714–7723.
- [12] S.S.V. Tatiparti, F. Ebrahimi, Electrodeposition of Al–Mg alloy powders, *J. Electrochem. Soc.* 155 (2008) D363–D368.
- [13] S.S.V. Tatiparti, F. Ebrahimi, An understanding of the electrodeposition process of Al–Mg alloys using an organometallic-based electrolyte, *J. Appl. Electrochem.* 40 (2010) 2091–2098.
- [14] S.S.V. Tatiparti, F. Ebrahimi, Internal structure of the electrodeposited nanocrystalline Al–Mg alloy dendrites, *Mater. Lett.* 65 (2011) 2413–2415.
- [15] S.S.V. Tatiparti, F. Ebrahimi, The formation of morphologies and microstructures in electrodeposited nanocrystalline Al–Mg alloy powders, *J. Electrochem. Soc.* 157 (2010) E167–E171.
- [16] S.S.V. Tatiparti, Extended solubility in the electrodeposited nanocrystalline Al–Mg alloy dendrites, *Mater. Lett.* 65 (2011) 3173–3175.
- [17] S.S.V. Tatiparti, Banded structure of the electrodeposited nanocrystalline Al–Mg alloy dendrites, *Mater. Lett.* 65 (2011) 3262–3264.
- [18] S.S.V. Tatiparti, F. Ebrahimi, Preferred orientation and shape of electrodeposited nanocrystalline Al–Mg alloy dendrites, *Mater. Lett.* 65 (2011) 1915–1918.
- [19] S.S.V. Tatiparti, F. Ebrahimi, Substrate effect on electrodeposited nanocrystalline Al–Mg alloy powders, *Mater. Lett.* 65 (2011) 1859–1861.
- [20] S.S.V. Tatiparti, F. Ebrahimi, Potentiostatic versus galvanostatic electrodeposition of nanocrystalline Al–Mg alloy powders, *J. Solid State Electrochem.* 16 (2012) 1255–1262.
- [21] S.S.V. Tatiparti, F. Ebrahimi, Evolution of morphology and microstructure in electrodeposited nanocrystalline Al–Mg alloy dendrites, *Metals* 1 (2011) 3–15.
- [22] J.L. Murray, The Al–Mg (Aluminum–Magnesium) system, *Bull. Alloy Phase Diagr.* 3 (1982) 60–74.

Sankara Sarma V. Tatiparti*

Materials Science and Engineering Department, University of Florida,
Gainesville, FL, 32611, USA

Department of Energy Science and Engineering, Indian Institute of
Technology Bombay, Mumbai, 400076, India

Fereshteh Ebrahimi

Materials Science and Engineering Department, University of Florida,
Gainesville, FL, 32611, USA

* Corresponding author. Department of Energy Science and
Engineering, Indian Institute of Technology Bombay, Mumbai,
400076, India

E-mail addresses: sankara@ufl.edu, sankara@iitb.ac.in (S.S.V.
Tatiparti).

24 July 2016

Available online 4 October 2016